

# Spin-torque contribution to the ac spin Hall conductivity

Arturo Wong, Jesús A. Maytorena, Catalina López-Bastidas, and Francisco Mireles

*Centro de Ciencias de la Materia Condensada, Departamento de Física Teórica, Universidad Nacional Autónoma de México, Apartado Postal 2681, 22800 Ensenada, Baja California, México*

(Received 13 July 2007; revised manuscript received 14 October 2007; published 2 January 2008)

Using the recently proposed definition of a conserved spin-current operator [J. Shi *et al.*, Phys. Rev. Lett. **96**, 076604 (2006)], we explore the frequency dependent spin Hall conductivity for a two-dimensional electron gas with Rashba and Dresselhaus spin-orbit interaction in response to an oscillating electric field. We show that the optical spectrum of the spin Hall conductivity exhibits remarkable changes when the definition of a conserved spin current is applied. Such behavior is mainly due to a significant contribution of the spin-torque term which is absent in the conventional form of the spin current. In addition, it is observed that the magnitude and direction of the dynamic spin Hall current strongly depend on the electric field frequency as with the interplay of the spin-orbit coupling strengths.

DOI: [10.1103/PhysRevB.77.035304](https://doi.org/10.1103/PhysRevB.77.035304)

PACS number(s): 72.25.-b, 72.25.Dc

## I. INTRODUCTION

The spin Hall effect (SHE) is a phenomenon that has motivated a very conspicuous interest among the semiconductor spintronics<sup>1,2</sup> researchers. The SHE refers to a spin accumulation induced via a driven spin current in response to a perpendicular dc electric field in finite width nonmagnetic systems which experiment spin-orbit interaction (SOI) effects.<sup>3-5</sup> This spin (Hall) accumulation with opposite spin magnetization at the edges of such systems has been beautifully demonstrated by recent optical experiments.<sup>6,7</sup> These observations were followed by purely electrical measurements of the SHE in metallic conductors<sup>8</sup> and by its very recent detection at room temperature via Kerr spectroscopy in *n*-type ZnSe samples.<sup>9</sup>

The role of disorder in the universal characteristic<sup>10</sup> of the dc spin Hall conductivity ( $e/8\pi$ ) in two-dimensional electron gases (2DEG's) with Rashba SOI has been central topic. Nowadays, there is a general consensus that the spin Hall conductivity is suppressed only in the static limit even in arbitrary weak disordered systems and as long as *k*-linear Rashba SOI is considered in infinite size samples.<sup>10-15</sup> This, however, does not hold in the presence of magnetic fields and/or magnetic impurities,<sup>10,16,17</sup> neither for two-dimensional (2D) hole systems<sup>18-20</sup> for which the static spin Hall conductivity is robust against disorder. Recently, Grimaldi *et al.*<sup>21</sup> have showed that this is also true when the Fermi energy is comparable to the spin-orbit splitting energy ( $E_F \sim \Delta$ ).

Yet, another possibility to gain further physical insight to the SHE is the finite frequency regime of transport.<sup>22</sup> Recent studies of the ac field-induced charge<sup>23</sup> and spin<sup>24</sup> response of 2DEG's have emphasized the importance of the dynamic regime.<sup>25</sup> It has been suggested that an ac probing field can be used to control the spin Hall current in 2DEG's with Rashba and/or Dresselhaus SOI.<sup>24,25</sup> It turns out that for finite frequencies (in the terahertz range), the cancellation of the intrinsic spin Hall effect due to impurity scattering<sup>26</sup> is no longer perfect and in principle the effect may survive.<sup>27</sup>

Sugimoto *et al.*,<sup>28</sup> on the other hand, have raised the question recently about the dependence of the vanishing of the

spin Hall conductivity  $\sigma_{sH}(0)$  on the actual definition of the spin-current operator used. This is certainly a fundamental issue that we extend here at the finite frequency regime of the spin Hall conductivity,  $\sigma_{sH}(\omega)$ . The widely *ad hoc* form used for the spin-current operator for an electronic system  $J_s = \frac{\hbar}{4}\{\sigma_z, v_y\}$ , where  $\sigma_z$  is the Pauli spin *z* component and  $v_y$  the electron velocity operator, has the desirable form that resembles the charge-current operator. In 2D hole gases, the conventional definition seems to be consistent with edge-spin accumulation experiments<sup>29</sup> as with measurements of optically injected spin-polarized currents in semiconductors.<sup>30</sup> However, it does not fulfill a simple continuity equation<sup>31-33</sup> and appears as incomplete in describing spin transport in systems with spin-orbit coupling.<sup>34</sup>

Many efforts to clarify this issue have gone into this direction lately.<sup>34-42</sup> It seems, nevertheless, an unsettled problem yet. Furthermore, the discussions have been focused, namely, in the zero frequency limit. In particular, the recent proposal by Shi *et al.*<sup>34</sup> of a dubbed unambiguous and proper definition of a “conserved” spin-current density is indeed physically appealing and certainly deserves a close examination. This definition adds to the conventional part  $\mathbf{J}_s$ , a spin source term (torque dipole density  $\mathbf{P}_\tau$ ) associated with the electron spin precessional motion with the total spin-current density defined as  $\mathcal{J}_s = \mathbf{J}_s + \mathbf{P}_\tau$ . Moreover, among other interesting properties, it ensures that a continuity equation  $\frac{\partial S_z}{\partial t} + \nabla \cdot \mathcal{J}_s = 0$  is always satisfied, with  $S_z = \frac{\hbar}{2}\Psi^\dagger \sigma_z \Psi$  describing the spin density. It is thus worth elucidating to what extent the use of this conserved spin-current operator provides new insight on the ac spin Hall conductivity response in 2D systems with SOI effects. Whether or not such a definition of the spin-current operator offers a physically satisfactory description of the ac spin Hall conductivity should be ultimately validated by the experiment.

In this paper, we study the ac spin Hall conductivity within the linear response theory employing the definition for the spin-current operator reported by Shi *et al.*<sup>34</sup> for a 2DEG in the presence of Rashba and Dresselhaus SOI and subject to an alternating electric field of frequency  $\omega$ . It is verified *post facto* that the optical spectrum of the spin Hall conductivity changes drastically when the definition is used

due to a nontrivial spin-torque contribution and to the interplay of the Rashba and Dresselhaus SOI. We predict that the torque dipole contribution to the ac spin Hall conductivity generally dominates over the conventional part in typical samples.

The work is organized as follows. In Sec. II, we describe the Hamiltonian model for a 2DEG in the presence of Rashba and Dresselhaus spin-orbit interaction. The main features of the Kubo formula in linear response applied to the spin Hall conductivity are presented in Sec. III. An analysis of the calculated ac spin Hall response using the conserved spin-current operator is presented also in this section. In Sec. IV, we give a discussion of the analytical and numerical results obtained for typical 2DEG systems. A summary is given in Sec. V and we end with a brief appendix which outlines the derivation of the spin-current-charge-current correlation function used in the Kubo formula.

## II. MODEL

We consider a 2D electron system with a single-particle Hamiltonian given by

$$H = \frac{p^2}{2m^*} + H_{so}, \quad (1)$$

where the spin-orbit part  $H_{so}$  is the sum of the Rashba and (linear) Dresselhaus SOI types with

$$H_{so} = \frac{\alpha}{\hbar}(\sigma_y p_x - \sigma_x p_y) + \frac{\beta}{\hbar}(\sigma_x p_x - \sigma_y p_y). \quad (2)$$

Here,  $\alpha$  and  $\beta$  are the coupling strengths for the Rashba and Dresselhaus couplings, respectively, with  $p_x, p_y$  the components of the 2D momentum operator and  $\sigma_x, \sigma_y$  the usual spin Pauli matrices. For the full Hamiltonian [Eq. (1)], the energy spectrum is simply

$$\varepsilon_\mu = \frac{\hbar^2 k^2}{2m^*} + \mu k \Delta(\theta) \quad (3)$$

with  $\mu \in \{+1, -1\}$  denoting the spin states for spin-split dispersion bands and  $\Delta(\theta) = \sqrt{(\alpha^2 + \beta^2)\lambda(\theta)}$  describes the angular anisotropy of the spectrum (see Fig. 1) with

$$\lambda(\theta) = 1 - \frac{2\alpha\beta}{\alpha^2 + \beta^2} \sin 2\theta, \quad (4)$$

and  $\theta = \tan^{-1}(\frac{k_y}{k_x})$ . When  $\alpha$  or  $\beta$  is null,  $\lambda(\theta) = 1$  and the spin splitting in  $k$  space becomes isotropic. The eigenstates have the form

$$|\psi_{\mathbf{k},\mu}(\mathbf{r})\rangle = \frac{e^{i\mathbf{k}\cdot\mathbf{r}}}{\sqrt{2A}} \begin{bmatrix} 1 \\ -\mu e^{-i\phi} \end{bmatrix}, \quad (5)$$

with the wave vector  $\mathbf{k} = (k_x, k_y) = k(\cos \theta, \sin \theta)$  in polar coordinates,  $\phi = \tan^{-1}(\frac{\alpha k_x - \beta k_y}{\alpha k_y - \beta k_x})$ , and  $A$  the area of the system. At zero temperature, the two spin-split subbands are filled up to the same (positive) Fermi energy level  $\varepsilon_F$  but with different Fermi wave vectors  $k_F^\mu(\theta) = \sqrt{\frac{2m^*\varepsilon_F}{\hbar^2} + k_{so}^2 \lambda(\theta) - \mu k_{so} \sqrt{\lambda(\theta)}}$ .

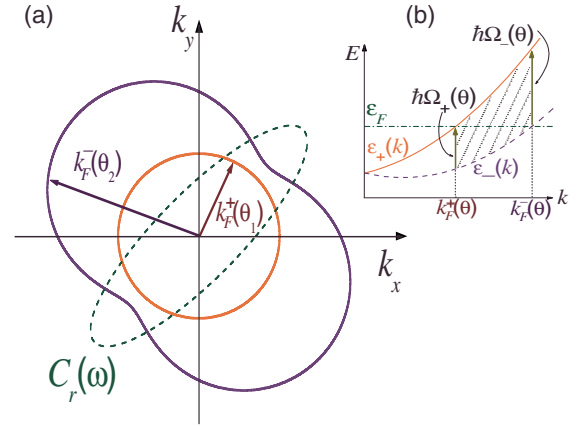


FIG. 1. (Color online) (a) Schematic diagram showing the angular anisotropy of the spin-split conduction bands at the Fermi energy in a 2DEG with finite Rashba and Dresselhaus spin-orbit interaction. The dotted  $C_r(\omega)$  curve is a rotated ellipse resulting from the condition  $\varepsilon_+(\mathbf{k}) - \varepsilon_-(\mathbf{k}) = \hbar\omega$ , see text for details. (b) Diagram depicting the allowed optical transitions (shaded region) between the initial  $\varepsilon_-$  and final  $\varepsilon_+$  spin-split branches at a fixed polar angle  $\theta$ .

Here,  $\varepsilon_F = \frac{\hbar^2 k_F^2}{2m^*}$  with  $k_F = \sqrt{2\pi n - 2k_{so}^2}$  and  $n$  being the electron density. The SOI introduces a characteristic SOI energy and wave vector given by  $\varepsilon_{so} = \frac{\hbar^2 k_{so}^2}{2m^*}$  and  $k_{so} = \frac{m^* \sqrt{\alpha^2 + \beta^2}}{\hbar^2}$ , respectively.

## III. SPIN HALL CONDUCTIVITY AT FINITE FREQUENCY

Within linear response to a weak (spatially homogeneous) electric field of frequency  $\omega$  oscillating in the plane of the 2DEG, the frequency dependent spin Hall conductivity can be calculated using the standard Kubo formula<sup>18</sup> in the limit  $q \rightarrow 0$ ,

$$\sigma_{xy}^{S,z}(\omega) = \frac{e}{\hbar A(\omega + i\eta)} \int_0^\infty e^{i(\omega + i\eta)t} \sum_{\mathbf{k}, \mu} f(\varepsilon_\mu)_{T=0} \langle \psi_{\mathbf{k},\mu}(\mathbf{r}) | \times [\mathcal{J}_x^{S,z}(t), v_y(0)] | \psi_{\mathbf{k},\mu}(\mathbf{r}) \rangle dt, \quad (6)$$

where we have assumed zero temperature and noninteracting carriers. The parameter  $\eta > 0$  is here to regularize the integral, but it can be viewed (phenomenologically) as a measure of the electron momentum dissipation effects due to impurity scattering events or any other many-body interactions<sup>18</sup> with an overall time-relaxation rate  $\tau = \eta^{-1}$  and  $f(\varepsilon_\mu)$  is the Fermi distribution function. Here, we employ the conserved spin-current operator of Shi *et al.*<sup>34</sup> written in the Heisenberg picture,  $\mathcal{J}_x^{S,z}(t)$ . Unlike the conventional definition  $J_s$ , the new effective spin current  $\mathcal{J}_s$  is (i) in conjugation with a mechanical or thermodynamical force (i.e., Onsager's reciprocity relations are well established), (ii) it has the desirable property that it vanishes for localized orbitals which anticipates a zero SHE for insulators, and (iii) predicts that the static value of spin Hall conductivity has an opposite sign to those reported using the conventional definition for Rashba

and linear Dresselhaus SOI models.<sup>34,39</sup> It is shown in Ref. 34, after imposing a null torque dipole density outside the bulk, that the effective spin-current operator  $\hat{\mathcal{J}}_s$  can be simply recasted as  $\hat{\mathcal{J}}_s = \frac{\hbar}{2} \frac{d(\hat{\sigma}_z)}{dt}$ . As a result, it adds an extra term which takes into account the spin-torque contribution.<sup>34</sup> In Eq. (6),  $v_y(0)$  is the single-particle operator for the electron velocity which can be obtained from the Heisenberg equation of motion  $\mathbf{v}(0) = \frac{i}{\hbar} [H, \mathbf{r}]$ . For our system, we get  $v_y(0) = \frac{p_y}{m} - \left( \frac{\alpha\sigma_x + \beta\sigma_y}{\hbar} \right)$ . The spin conductivity  $\sigma_{xy}^{S,z}(\omega)$  in Eq. (6) describes a  $z$ -polarized spin current flowing in the  $x$  direction as a function of frequency  $\omega$  in response to a weak electric field  $E(\omega)$  chosen along the  $y$  direction.

To obtain explicitly  $\mathcal{J}_x^{S,z}(t)$ , we first take the  $x$  component of the current operator with a spin moment polarized along the  $z$  direction at time  $t=0$  (via the Heisenberg equation of motion), yielding

$$\mathcal{J}_x^{S,z}(0) = \frac{\hbar}{2m^*} \sigma_z p_x + \left[ \hat{x}, \frac{\beta}{2\hbar} (\sigma_x p_y + \sigma_y p_x) - \frac{\alpha}{2\hbar} (\sigma_x p_x + \sigma_y p_y) \right], \quad (7)$$

where the symbol  $\{\cdot\}$  denotes the anticommutator. The first term in Eq. (7) represents the conventional spin-current part, while the second term arises entirely from the spin-torque contribution.

It can be shown that the expected value of the spin-current-charge-current correlation function in Eq. (6)  $\langle \psi_{\mathbf{k},\mu}(\mathbf{r}) | [\mathcal{J}_x^{S,z}(t), v_y(0)] | \psi_{\mathbf{k},\mu}(\mathbf{r}) \rangle \equiv \mathcal{F}_\mu(\mathbf{k}, t)$  takes the form (see Appendix)

$$\mathcal{F}_\mu(\mathbf{k}, t) = i\mu \frac{\hbar k_x^2 (\beta^2 - \alpha^2)}{m^* k \Delta(\theta)} \left\{ \cos \left[ \frac{2k\Delta(\theta)}{\hbar} t \right] - \frac{2k\Delta(\theta)}{\hbar} t \sin \left[ \frac{2k\Delta(\theta)}{\hbar} t \right] \right\}. \quad (8)$$

By using this result in Eq. (6) together with the fact that  $\sum_{\mathbf{k},\mu} \mu f(\varepsilon_\mu)_{T=0} = -\sum_{\mathbf{k}} \Theta[(k - k_F^+)(k_F^- - k)]$ , where  $\Theta(x)$  is the Heaviside step function, it is then possible to decompose the frequency dependent spin conductivity into the sum of two terms, namely,

$$\sigma_{xy}^{S,z}(\omega) = \sigma_c^{SH}(\omega) + \sigma_\tau^{SH}(\omega), \quad (9)$$

in which the first one is given by

$$\sigma_c^{SH}(\omega) = \frac{e(\beta^2 - \alpha^2)}{4\pi^2 m^*} \int_0^{2\pi} d\theta \frac{\cos^2 \theta}{\Delta(\theta)} \times \int_{k_F^-(\theta)}^{k_F^+(\theta)} dk \frac{k^2}{(\omega + i\eta)^2 - [2k\Delta(\theta)/\hbar]^2} \quad (10)$$

and comes from the conventional part of spin-current definition. The second term is explicitly

$$\sigma_\tau^{SH}(\omega) = \frac{e(\beta^2 - \alpha^2)}{4\pi^2 m^*} \int_0^{2\pi} d\theta \frac{8 \cos^2 \theta \Delta(\theta)}{\hbar^2} \times \int_{k_F^-(\theta)}^{k_F^+(\theta)} dk \frac{k^4}{\{(\omega + i\eta)^2 - [2k\Delta(\theta)/\hbar]^2\}^2} \quad (11)$$

and arises from the spin-torque contribution to the net spin current. As a general trend, it will be shown later that such contribution introduces a significant change of the spin Hall optical response overcoming the conventional part for typical sample parameters.

At this stage, it is worthwhile to remark that in the limit  $\omega\tau \rightarrow \infty$ , the impurity scattering does not play a significant role in spin transport.<sup>10</sup> Indeed, in the language of the diagrammatic technique, the resulting finite vertex corrections are negligible in the weak scattering limit for the ac high frequency field regime. This occurs because in linear response to the ac field, the perturbative expansion in powers of  $n_i$  (impurity density) of the spin-current-charge-current correlation function goes as  $1/(\omega\tau)^n$ , which makes the contribution of the vertex corrections vanish at high frequencies.<sup>10,24</sup> Thus, the linear response Kubo calculation without including explicitly the vertex corrections should give a qualitatively good agreement with the full diagrammatic technique at high enough frequencies and low impurity densities.<sup>24</sup>

The  $k$  integration in expressions (10) and (11) can be done analytically, yielding for the conventional part of spin conductivity

$$\frac{\sigma_c^{SH}(\omega)}{e/8\pi} = \frac{1}{\pi} \frac{\alpha^2 - \beta^2}{\alpha^2 + \beta^2} \int_0^{2\pi} \frac{\cos^2(\theta)}{\lambda(\theta)} \times \left\{ 1 + \frac{\hbar\tilde{\omega}}{8\varepsilon_{so}\lambda(\theta)} \tanh^{-1} \left[ \frac{8\varepsilon_{so}\lambda(\theta)\hbar\tilde{\omega}}{16\varepsilon_F\varepsilon_{so}\lambda(\theta) - \hbar^2\tilde{\omega}^2} \right] \right\} d\theta, \quad (12)$$

where  $\tilde{\omega} = \omega + i\eta$  and  $\lambda(\theta)$  as is defined in Eq. (4). The torque contribution becomes

$$\frac{\sigma_\tau^{SH}(\omega)}{e/8\pi} = -\frac{1}{\pi} \frac{\alpha^2 - \beta^2}{\alpha^2 + \beta^2} \int_0^{2\pi} \frac{\cos^2(\theta)}{\lambda(\theta)} \times \left\{ 2 + \frac{3\hbar\tilde{\omega}}{8\varepsilon_{so}\lambda(\theta)} \tanh^{-1} \left[ \frac{8\varepsilon_{so}\lambda(\theta)\hbar\tilde{\omega}}{16\varepsilon_F\varepsilon_{so}\lambda(\theta) - \hbar^2\tilde{\omega}^2} \right] + \frac{[16\varepsilon_F\varepsilon_{so}\lambda(\theta) + \hbar^2\tilde{\omega}^2]\hbar^2\tilde{\omega}^2}{[16\varepsilon_F\varepsilon_{so}\lambda(\theta) - \hbar^2\tilde{\omega}^2]^2 - 64\varepsilon_{so}^2\lambda^2(\theta)\hbar^2\tilde{\omega}^2} \right\} d\theta. \quad (13)$$

Note that if  $\beta=0$  (or  $\alpha=0$ ), i.e., if  $\lambda(\theta)=1$ , the angular dependence of the integrand above reduces significantly and leads to a close analytic form for  $\sigma_c^{SH}(\omega)$  and  $\sigma_\tau^{SH}(\omega)$ . For the case  $\alpha \neq \beta$ , the  $\theta$  integrals cannot be performed straightforwardly and a numerical integration has to be implemented. Thus, it is convenient to consider first the physically reasonable limit  $k_{so} \ll k_F$ , which typically holds for 2DEGs in III-V-based semiconductor heterostructures and for which an

analytical expression for the frequency dependent spin conductivity can be derived.

From Eqs. (10) and (11), we obtain to leading order in  $k_{so}/k_F$ ,

$$\sigma_{xy}^{S,z}(\omega) \approx \sigma_{c,o}^{sH}(\omega) + \sigma_{\tau,o}^{sH}(\omega), \quad (14)$$

in which the conventional part reads

$$\frac{\sigma_{c,o}^{sH}(\omega)}{e/8\pi} = -\frac{16(\beta^2 - \alpha^2)}{(\beta^2 + \alpha^2)} \frac{\varepsilon_F \varepsilon_{so}}{\prod_{\mu} [\xi_{\mu}^2 - \hbar^2 \tilde{\omega}^2]^{1/2}}, \quad (15)$$

while the spin-torque part takes the form

$$\begin{aligned} \frac{\sigma_{\tau,o}^{sH}(\omega)}{e/8\pi} = & \frac{32(\beta^2 - \alpha^2)}{(\beta^2 + \alpha^2)} \left[ \frac{\varepsilon_F \varepsilon_{so}}{\prod_{\mu} [\xi_{\mu}^2 - \hbar^2 \tilde{\omega}^2]^{1/2}} \right. \\ & \left. + \frac{\varepsilon_F \varepsilon_{so} \hbar^2 \tilde{\omega}^2 [16\varepsilon_F \varepsilon_{so} - \hbar^2 \tilde{\omega}^2]}{\prod_{\mu} [\xi_{\mu}^2 - \hbar^2 \tilde{\omega}^2]^{3/2}} \right], \end{aligned} \quad (16)$$

with  $\xi_{\mu} = 2k_F |\alpha + \mu\beta|$ .

Our result [Eq. (15)] agrees with Eq. (39) of Ref. 43 obtained there via the spin-susceptibility calculation.<sup>44</sup> Note also that the second term of Eq. (16) vanishes for  $\tilde{\omega}=0$ , while the first one, when added to Eq. (15), reverses the sign of the static value of the spin Hall conductivity [Eq. (14)]. On the other hand, it will be seen that, at finite frequencies, the torque dipole contribution of Shi *et al.*<sup>34</sup> generally dominates over the conventional spin-current contribution.

It is illustrative to analyze the behavior of the spin-Hall conductivity in the static limit ( $\omega=0$ ) in the presence of weak disorder when the conserved spin-current operator is applied. In particular, from Eqs. (15) and (16), the static value, for the pure Rashba coupling case, can be written in the appealing form as

$$\frac{\sigma_{xy}^{S,z}(0)}{e/8\pi} = \frac{\eta/\eta_{so} - 1}{(\eta/\eta_{so} + 1)^2}, \quad (17)$$

where  $\eta_{so} = \tau_{so}^{-1}$ ,  $\tau_{so}$  being the Dyakonov-Perel spin-orbit relaxation time<sup>45</sup> with  $\tau_{so}^{-1} = \frac{(2\alpha k_F/\hbar)^2}{\tau^{-1}}$ . Since  $\eta$  is typically smaller than  $\eta_{so}$  (i.e.,  $2\alpha k_F > \hbar\eta$ ), note that the static value of  $\sigma_{xy}^{S,z}$  is always negative.

It is known, however, that the dc limit is problematic within the Kubo formula when using the conventional spin-current operator, namely, because it leads to the incorrect physics for  $\varepsilon_{so} \gg \hbar\eta$  as a result of neglecting the contribution of the vertex corrections. This is not necessarily the case for finite frequencies and relatively low impurity densities (as discussed below), which is, in fact, the regime that we are mostly interested in here. In the opposite limit,  $\varepsilon_{so} \ll \hbar\eta$ , the Kubo formula gives a result which coincides qualitatively with the expected result.<sup>18</sup> We first consider this case. Taking the limit  $\omega \rightarrow 0$  for finite but weak scattering mechanism with a time-relaxation rate  $\tau^{-1} = \eta$  and expanding Eqs. (15) and (16) in powers of  $\varepsilon_{so}/\hbar\eta \ll 1$  to lowest order, we get

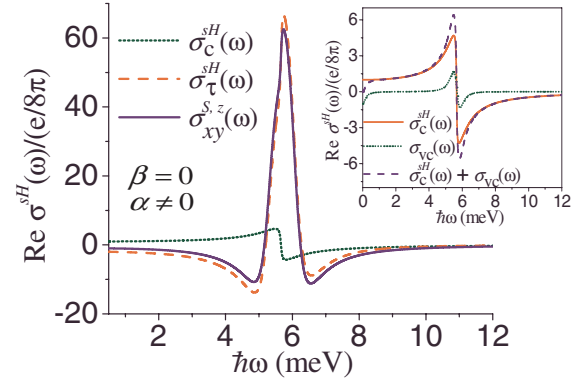


FIG. 2. (Color online) Real part of the spin Hall conductivity as a function of the photon energy for a 2DEG system with Rashba SOI only ( $\beta=0$ ). The dotted curve is obtained using the conventional definition of spin current, whereas the dashed and solid curves are the torque contribution and the total spin conductivity, respectively, employing the conserved spin-current operator. In the inset, the result obtained taking into account vertex corrections is contrasted with our calculations (see text for parameter values used).

$$\frac{\sigma_{c,o}^{sH}(0)}{e/8\pi} \approx \frac{\alpha^2 - \beta^2}{\alpha^2 + \beta^2} \left( \frac{16\varepsilon_F \varepsilon_{so}}{\hbar^2 \eta^2} \right), \quad (18)$$

while  $\sigma_{\tau,o}^{sH}(0) = 0$ .

Now, if the impurity scattering is weak compared to the spin-orbit coupling,  $\varepsilon_{so}/\hbar\eta \gg 1$ , we obtain to first order,

$$\frac{\sigma_{c,o}^{sH}(0)}{e/8\pi} \approx \left[ 1 - \frac{\hbar^2 \eta^2}{16\varepsilon_F \varepsilon_{so}} \frac{(\alpha^2 + \beta^2)^2}{(\alpha^2 - \beta^2)^2} \right] \text{sgn}(\alpha^2 - \beta^2) \quad (19)$$

with a nonzero torque part

$$\frac{\sigma_{\tau,o}^{sH}(0)}{e/8\pi} \approx \left[ -2 + \frac{\hbar^2 \eta^2}{4\varepsilon_F \varepsilon_{so}} \frac{(\alpha^2 + \beta^2)^2}{(\alpha^2 - \beta^2)^2} \right] \text{sgn}(\alpha^2 - \beta^2). \quad (20)$$

The above expressions for  $\sigma_{c,o}^{sH}(0)$  reduce, in each case, to the known formulas for  $\beta=0$  reported in Ref. 18.

#### IV. RESULTS AND DISCUSSIONS

We first study the case where only the Rashba coupling is present ( $\beta=0$ ). In Fig. 2, we plot the real part of the spin Hall conductivity versus the frequency of the applied electric field as obtained from Eqs. (12) and (13) [ $\lambda(\theta)=1$ ]. The Rashba parameter has been fixed to  $\alpha = 1.6 \times 10^{-9}$  eV cm, which is a typical experimental value for a 2DEG in InAs-based quantum wells. Using an electron effective mass of  $m^* = 0.055m_o$ , these values give us a characteristic Rashba energy of  $\varepsilon_{so} = 0.092$  meV with a spin splitting at the Fermi energy of  $\Delta_R = 2\alpha k_F \approx 5.6$  meV. The corresponding Fermi wave number is estimated with  $k_F = \sqrt{2\pi n}$  considering a moderated sheet electron density of  $n = 5 \times 10^{11}$  cm<sup>-2</sup>. The parameter describing the momentum relaxation rate has been chosen such that  $\hbar\eta = 0.4$  meV, a value that corresponds to high quality samples with mobilities  $\mu = e\tau/m^* \approx 5$  m<sup>2</sup>/V s and relaxation times of  $\tau \approx 1.6$  ps. We have plotted as a ref-



erence (dotted curve in Fig. 1) the result obtained using the conventional definition of spin current [Eq. (10)].

The spin Hall conductivity  $\sigma_c^{sH}(\omega)$  shows resonance behavior at energies  $\hbar\omega_+ \approx 2\alpha k_F$  and  $\hbar\omega_- \approx 2\alpha k_F$ , which correspond, respectively, to the minimum and maximum photon energies required to induce optical transitions between the initial  $\mu=-1$  and final  $\mu=+1$  spin-split branches (see Fig. 1). At low frequencies, it approaches the universal value  $e/8\pi$ , while it vanishes for high frequencies. Because of the finite value of the damping parameter  $\eta$ , the spectrum has a smoothed shape across the shifted resonance frequencies  $\omega'_\pm = \sqrt{\omega_\pm^2 + \eta^2}$ . Notice that for  $k_{so} \ll k_F$ , the approximated solution of  $\sigma_{c,o}^{sH}(\omega)$  in Eq. (15) will give nearly the same numerical values with slightly shifted resonance frequencies at  $\omega'_\pm \approx \sqrt{\omega_\pm^2 + 2\eta^2 \sqrt{(\Delta_R/\hbar\eta)^2 + 1}}$ , where  $\eta > 0$  is understood and  $\omega_o = \eta \sqrt{(\Delta_R/\hbar\eta)^2 + 1}$  is the intermediate frequency at which the conventional part vanishes.

For the sake of contrast, the inset of Fig. 1 shows the behavior of the conventional part of the spin Hall conductivity [Eq. (10)] and that obtained from expression (21) of Ref. 13 which incorporates explicitly the vertex corrections. It is shown that at finite high frequencies ( $\hbar\omega \gtrsim 0.5$  meV), the result obtained neglecting the vertex corrections reproduces qualitatively the expected behavior, being in quite good agreement for finite frequencies outside the corresponding energy window referred above, that is, for  $\omega \gtrsim \omega'_-$  and  $\omega \lesssim \omega'_+$ .

As for the effect of the torque dipole contribution on the spin Hall conductivity, we notice that the first two terms in expression (13) change the sign of the terms giving  $\sigma_c^{sH}(\omega)$  in Eq. (12), when added to obtain the total conductivity  $\sigma_{xy}^{s,z}(\omega)$ . On the other hand, the last term of  $\sigma_\tau^{sH}(\omega)$  [Eq. (13)] is a rational function which can be rewritten (for  $\beta=0$  and  $\tilde{\omega} \neq 0$ ) as

$$-\frac{(\tilde{\omega}^2 + \Delta_R^2/\hbar^2)(\tilde{\omega}^2 + 4\varepsilon_R^2/\hbar^2)}{(\tilde{\omega}^2 - \omega_+^2)(\tilde{\omega}^2 - \omega_-^2)}, \quad (21)$$

where  $\varepsilon_R = 2\varepsilon_{so} = m^* \alpha^2/\hbar^2$ . As shown in Fig. 2, this contribution dominates the shape of the spectrum. It also resonates at the (shifted) frequencies  $\omega'_\pm$ , being positive for  $\omega$  between  $\omega'_+$  and  $\omega'_-$ , and negative otherwise. Consequently, a dramatic change of the overall shape of the spectrum is observed. This is one of the main results of this paper. By measuring if possible, the spin Hall current and/or spin accumulation at low temperatures in the frequency domain, it could be helpful, perhaps, to establish the validity of the definition of the spin-current operator proposed by Shi *et al.*<sup>34</sup> by contrasting with our results.

Interesting features appear when the interplay of the Rashba and Dresselhaus SOI is considered. In Fig. 3(a), we plot the frequency dependent spin Hall conductivity for  $\beta = 0.5\alpha$ ; here,  $\hbar\eta = 0.25$  meV and the remaining parameters are as in Fig. 2. The results using the approximated formulas (15) and (16) and the exact numerical integration of Eqs. (12) and (13) is presented for comparison. Here, the remarkable difference between the optical spectrum resulting from the use of the standard and the conserved spin-current opera-

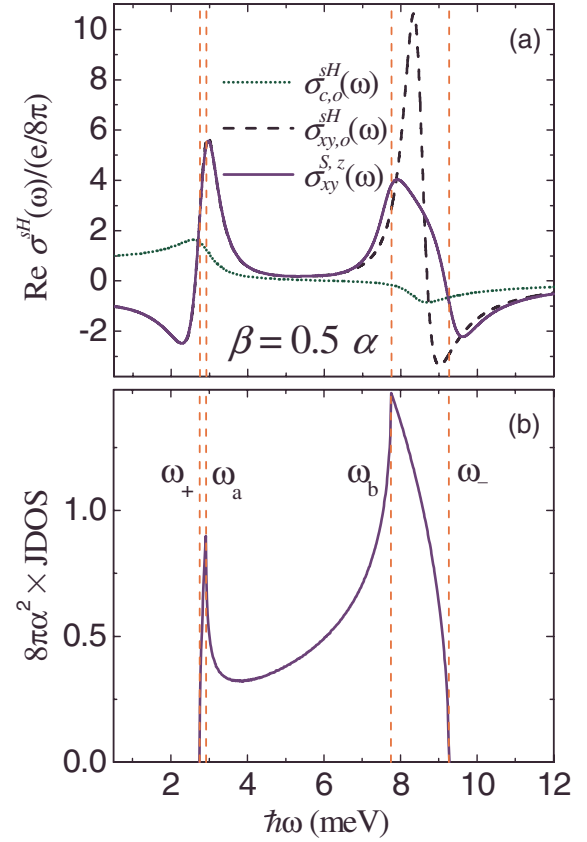


FIG. 3. (Color online) (a) Frequency dependent spin Hall conductivity for a 2DEG system with finite Rashba and Dresselhaus SOI ( $\beta=0.5\alpha$ ), employing the conventional definition of spin current (dotted curve), the conserved spin-current operator  $\mathcal{J}_{xy}^{s,z}$  in the limit  $k_{so} \ll k_F$  (dashed curve), and the exact numerical integration of Eq. (6) (solid curve). Here,  $\hbar\eta=0.25$  meV and other parameters as in Fig. 2(b). Plot for the corresponding joint density of states (JDOS). There are four main frequencies here, two defining the optical absorption edges,  $\omega_-$  and  $\omega_+$ , while the other two correspond to the peaks of the JDOS occurring at  $\omega_a$  and  $\omega_b$ . The latter two arises due to the symmetry of the spin-split conduction bands in  $k$  space at the Fermi level. The dashed vertical lines at the frequencies referred above are here to guide eyes.

tor definition,  $\mathcal{J}_x^{s,z}$ , is also evident. In addition, the spectra become wider and highly asymmetric in comparison with those of the  $\beta=0$  or  $\alpha=0$  case. As was recently discussed in Ref. 25, the main spectral features can be understood as due to the anisotropic spin splitting caused by the simultaneous presence of the Rashba and Dresselhaus couplings. In the limit of vanishing temperature, the sum over states in Eq. (6) is restricted to the region between the Fermi contours  $k_F^+(\theta) \leq k \leq k_F^-(\theta)$ , for which  $\varepsilon_-(k, \theta) \leq \varepsilon_F \leq \varepsilon_+(k, \theta)$  (see Fig. 1). Certain distinctive frequencies can be identified given the anisotropic  $k$  space available for the optical response. To illustrate this, we consider the joint density of states (JDOS) for the spin-split branches [Fig. 3(b)], which gives the number of direct transitions that can take place at the energy  $\hbar\omega$ . These transitions involve only states with wave vectors that satisfy the equation  $\varepsilon_+(k, \theta) - \varepsilon_-(k, \theta) - \hbar\omega = 0$ , which for a fixed photon energy defines a curve  $C_r(\omega)$  in  $k$  space describ-

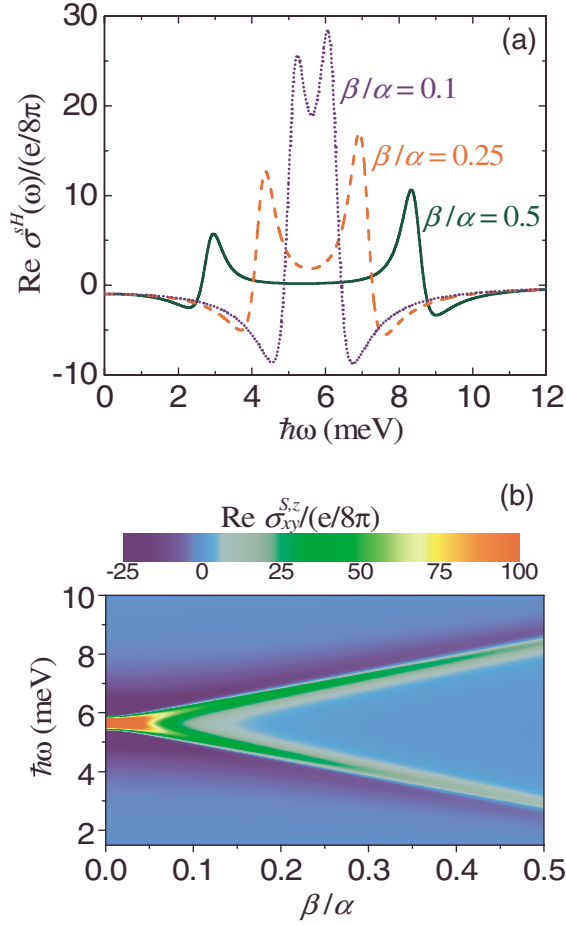


FIG. 4. (Color online) (a) Spin Hall conductivity for  $\beta/\alpha = 0.5, 0.25, 0.1$  (solid, dashed, and dotted curves, respectively) with the proposed conserved spin-current operator  $\mathcal{J}_{xy}^{S,z}$ . The parameters are as in Fig. 2 with  $\hbar\eta = 0.25$  meV. Notice that the resonance peaks tend to separate in energy as the ratio  $\beta/\alpha$  is increased while its magnitude is diminished. (b) Color contour map of the ac spin Hall conductivity showing its behavior with a continuous variation of the frequency  $\omega$  and to the ratio  $\beta/\alpha$ .

ing a rotated ellipse with semiaxis of lengths  $k_a(\omega) = \hbar\omega/2|\alpha - \beta|$  and  $k_b(\omega) = \hbar\omega/2|\alpha + \beta|$  oriented along the principal axes (1,1) and (-1,1), respectively (see Fig. 1). Thus, for our problem, the JDOS involves states only along the arcs of the resonance curve  $C_r(\omega)$  lying within the mentioned region  $k_F^+(\theta) \leq k \leq k_F^-(\theta)$ . The peaks observed in the JDOS correspond to energy transitions involving states in the vicinity of the symmetry points  $k_a(\omega) = k_F^-(\pi/4)$  and  $k_b(\omega) = k_F^+(3\pi/4)$ , for which the energy splitting reaches extreme values. These equations determine two energies  $\hbar\omega_a = 2k_F^-(\pi/4)|\alpha - \beta| = 2k_F|\alpha - \beta| + 2m^*(\alpha - \beta)^2/\hbar^2$  and  $\hbar\omega_b = 2k_F^+(3\pi/4)|\alpha + \beta| = 2k_F|\alpha + \beta| - 2m^*(\alpha + \beta)^2/\hbar^2$ . Similarly, we can see that there are absorption edges at energies  $\hbar\omega_{\pm} = 2k_F|\alpha \mp \beta| \mp 2m^*(\alpha \mp \beta)^2/\hbar^2$ , corresponding to transitions between states at the points  $k_a(\omega) = k_F^-(\pi/4)$  and  $k_b(\omega) = k_F^+(3\pi/4)$ . For clarity, such energies are indicated in Fig. 3 with dashed vertical lines. As expected, the spin Hall conductivity  $\sigma_{xy}^{S,z}(\omega)$  also shows a structure at the photon energies  $\hbar\omega_{\pm}$ ,  $\hbar\omega_a$ , and  $\hbar\omega_b$ . The finite value of  $\hbar\eta$  chosen here

yields a slight shifting of these energies and an overall smoothing of the spectrum.

It is clear that the definition of the spin-current operator by Shi *et al.*<sup>34</sup> yields a dramatically different frequency response from that predicted by the conventional definition. In addition, as it occurs with the pure Rashba (or Dresselhaus) SOI case, the torque dipole contribution (not shown) turns out to be the dominant term in the spin Hall conductivity. Notice that the spectra in Fig. 3(a) show that the magnitude and the direction of the dynamic spin Hall current strongly depend on the frequency and on the spin-orbit coupling strengths  $\alpha$  and  $\beta$ , suggesting thus its control via electrical gating (by varying the Rashba coupling) and/or by adjusting the electric field frequency.

We have also explored the effect induced of varying the ratio  $\beta/\alpha$  on the conserved spin-Hall conductivity as a function of the exciting frequency. In particular, in Fig. 4(a), the spin Hall response is shown for the specific values of  $\beta/\alpha = 0.5, 0.25$ , and  $0.1$  while fixing the rest of the parameters, as in Fig. 3. Notice that the energy separation of the resonance peaks becomes larger and the intensity of the peaks gets diminished as the aspect ratio  $\beta/\alpha$  is increased. Such effect is emphasized in Fig. 4(b) where a color map of the spin Hall conductivity is plotted as a function of a continuous variation of the ratio  $\beta/\alpha$  and  $\omega$ . Such behavior responds to the wide-spreading ( $\Delta\mathcal{E} = \hbar\omega_- - \hbar\omega_+$ ) of absorption bandwidth with  $\beta$ .<sup>25</sup>

## V. SUMMARY

In summary, we have examined the spin Hall conductivity in the frequency regime for a two-dimensional electron gas with Rashba and Dresselhaus spin-orbit interaction employing a recently proposed form for a conserved spin-current operator. Our results shows that the optical spectrum of the spin Hall conductivity changes substantially when the conserved spin-current operator is used. It is predicted that the torque dipole contribution typically overcomes the conventional part of the total spin Hall conductivity. In addition, it is shown that the magnitude and the direction of the dynamic spin Hall current is rather sensitive to the frequency and to the spin-orbit ( $\alpha$  and  $\beta$ ) coupling strengths due to the spin torque contribution. We hope that these results will encourage experimentalists to measure the spin Hall accumulation and/or spin density currents and to explore to what extent the new definition of the spin-current operator provides a satisfactory description of the ac spin Hall conductivity in such systems.

## ACKNOWLEDGMENTS

F.M. is thankful to Q. Niu for useful comments. This work was supported by CONACyT-Mexico Grant No. J41113F and by DGAPA-UNAM IN113807-3.

## APPENDIX

Here, we briefly outline the derivation of the expectation value for spin-current-charge-current correlation function

$\langle \psi_{\mathbf{k},\mu}(\mathbf{r}) | [\mathcal{J}_x^{\mathcal{S},z}(t), v_y(0)] | \psi_{\mathbf{k},\mu}(\mathbf{r}) \rangle \equiv \mathcal{F}_\mu(\mathbf{k}, t)$ . We begin by writing the spin-current operator at all times in the Heisenberg picture,  $\mathcal{J}_x^{\mathcal{S},z}(t) = e^{iHt/\hbar} \mathcal{J}_x^{\mathcal{S},z}(0) e^{-iHt/\hbar}$ , with  $\mathcal{J}_x^{\mathcal{S},z}(0)$  as given by Eq. (7). This is similarly done for the operators  $x(t)$ ,  $\sigma_x(t)$ , and  $\sigma_y(t)$ , which after some algebraic manipulations explicitly reads,

$$x(t) = x(0) + t \left( \frac{p_x}{m} + \frac{\alpha\sigma_y + \beta\sigma_x}{\hbar} \right) + \frac{\hbar}{2\Delta^2 p^2} (\beta^2 - \alpha^2) p_y \sigma_z \left[ \cos\left(\frac{2\Delta p}{\hbar^2} t\right) - 1 \right] - \frac{\hbar}{2\Delta^3 p^3} (\beta^2 - \alpha^2) p_y \left[ \frac{2t\Delta p}{\hbar^2} - \sin\left(\frac{2\Delta p}{\hbar^2} t\right) \right] \mathcal{K}, \quad (\text{A1})$$

$$\sigma_x(t) = \sigma_x(0) + \frac{(\alpha p_x - \beta p_y)}{\Delta p} \sigma_z \sin\left(\frac{2\Delta p}{\hbar^2} t\right) - \frac{(\alpha p_x - \beta p_y)}{\Delta^2 p^2} \left[ \cos\left(\frac{2\Delta p}{\hbar^2} t\right) - 1 \right] \mathcal{K}, \quad (\text{A2})$$

and

$$\sigma_y(t) = \sigma_y(0) - \frac{(\beta p_x - \alpha p_y)}{\Delta p} \sigma_z \sin\left(\frac{2\Delta p}{\hbar^2} t\right) - \frac{(\beta p_x - \alpha p_y)}{\Delta^2 p^2} \left[ \cos\left(\frac{2\Delta p}{\hbar^2} t\right) - 1 \right] \mathcal{K} \quad (\text{A3})$$

with  $\mathcal{K} = \alpha(\sigma_x p_x + \sigma_y p_y) - \beta(\sigma_x p_y + \sigma_y p_x)$ , and in which  $\vec{\sigma}$  and  $\vec{p}$  are given in the Schrödinger picture. The expressions above are needed in the calculation of the commutator  $[\mathcal{J}_x^{\mathcal{S},z}(t), v_y(0)]$ , which gives

$$[\mathcal{J}_x^{\mathcal{S},z}(t), v_y(0)] = \frac{(\alpha\sigma_x + \beta\sigma_y)}{2m^*} e^{iHt/\hbar} \sigma_z p_x e^{-iHt/\hbar} - e^{iHt/\hbar} \sigma_z p_x e^{-iHt/\hbar} \frac{(\alpha\sigma_x + \beta\sigma_y)}{2m^*} + i[x(0), \mathcal{L}] + \frac{2itp_x}{m^*} \mathcal{L} \quad (\text{A4})$$

with  $\mathcal{L} = \frac{\Delta p}{\hbar^2} (\alpha\sigma_y - \beta\sigma_x) \sin\left(\frac{2\Delta p}{\hbar^2} t\right) + \frac{\sigma_z}{\hbar^2} \mathcal{P} \cos\left(\frac{2\Delta p}{\hbar^2} t\right)$  and  $\mathcal{P} = 2\alpha\beta p_x - (\alpha^2 + \beta^2) p_y$ . Calculating the expectation value of Eq. (A4) using Eq. (5), we finally arrive to  $\mathcal{F}_\mu(\mathbf{k}, t)$  as defined in Eq. (8).

- 
- <sup>1</sup>S. A. Wolf, D. D. Awschalom, R. A. Buhrman, J. M. Daughton, S. von Molnár, M. L. Roukes, A. Y. Chtchelkanova, and D. M. Treger, *Science* **294**, 1448 (2001).  
<sup>2</sup>I. Žutić, J. Fabian, and S. Das Sarma, *Rev. Mod. Phys.* **76**, 323 (2004).  
<sup>3</sup>J. E. Hirsch, *Phys. Rev. Lett.* **83**, 1834 (1999).  
<sup>4</sup>S. Murakami, N. Nagaosa, and S.-C. Zhang, *Science* **301**, 1348 (2003).  
<sup>5</sup>J. Sinova, D. Culcer, Q. Niu, N. A. Sinitsyn, T. Jungwirth, and A. H. MacDonald, *Phys. Rev. Lett.* **92**, 126603 (2004); N. A. Sinitsyn, E. M. Hankiewicz, W. Teizer, and J. Sinova, *Phys. Rev. B* **70**, 081312(R) (2004).  
<sup>6</sup>J. Wunderlich, B. Kaestner, J. Sinova, and T. Jungwirth, *Phys. Rev. Lett.* **94**, 047204 (2005).  
<sup>7</sup>Y. K. Kato, R. C. Myers, A. C. Gossard, and D. D. Awschalom, *Science* **306**, 1910 (2004).  
<sup>8</sup>S. O. Valenzuela and M. Tinkham, *Nature (London)* **442**, 176 (2006).  
<sup>9</sup>N. P. Stern, S. Ghosh, G. Xiang, M. Zhu, N. Samarth, and D. D. Awschalom, *Phys. Rev. Lett.* **97**, 126603 (2006).  
<sup>10</sup>J. Sinova, S. Murakami, S.-Q. Shen, and M.-S. Choi, *Solid State Commun.* **138**, 214 (2006).  
<sup>11</sup>J. I. Inoue, G. E. W. Bauer, and L. W. Molenkamp, *Phys. Rev. B* **70**, 041303(R) (2004).  
<sup>12</sup>E. G. Mishchenko, A. V. Shytov, and B. I. Halperin, *Phys. Rev. Lett.* **93**, 226602 (2004).  
<sup>13</sup>O. Chalaev and D. Loss, *Phys. Rev. B* **71**, 245318 (2005).  
<sup>14</sup>O. V. Dimitrova, *Phys. Rev. B* **71**, 245327 (2005).  
<sup>15</sup>R. Raimondi and P. Schwab, *Phys. Rev. B* **71**, 033311 (2005).  
<sup>16</sup>J. I. Inoue, T. Kato, Y. Ishikawa, H. Itoh, G. E. W. Bauer, and L. W. Molenkamp, *Phys. Rev. Lett.* **97**, 046604 (2006).  
<sup>17</sup>P. Wang, Y.-Q. Li, and X. Zhao, *Phys. Rev. B* **75**, 075326 (2007).  
<sup>18</sup>J. Schliemann and D. Loss, *Phys. Rev. B* **69**, 165315 (2004).  
<sup>19</sup>B. A. Bernevig and S.-C. Zhang, *Phys. Rev. Lett.* **95**, 016801 (2005).  
<sup>20</sup>A. Khaetskii, *Phys. Rev. B* **73**, 115323 (2006).  
<sup>21</sup>C. Grimaldi, E. Cappelluti, and F. Marsiglio, *Phys. Rev. B* **73**, 081303(R) (2006).  
<sup>22</sup>E. Ya. Sherman, A. Najmaie, and J. E. Sipe, *Appl. Phys. Lett.* **86**, 122103 (2005); E. I. Rashba, *Phys. Rev. B* **70**, 161201(R) (2004).  
<sup>23</sup>W. Xu, *Appl. Phys. Lett.* **82**, 724 (2003); D. W. Yuan, W. Xu, Z. Zeng, and F. Lu, *Phys. Rev. B* **72**, 033320 (2005); C. Zhang and Z. Ma, *ibid.* **71**, 121307(R) (2005).  
<sup>24</sup>C. M. Wang, S. Y. Liu, and X. L. Lei, *Phys. Rev. B* **73**, 035333 (2006).  
<sup>25</sup>J. A. Maytorena, C. López-Bastidas, and F. Mireles, *Phys. Rev. B* **74**, 235313 (2006).  
<sup>26</sup>A. Khaetskii, *Phys. Rev. Lett.* **96**, 056602 (2006).  
<sup>27</sup>A. Shekhter, M. Khodas, and A. M. Finkel'stein, *Phys. Rev. B* **71**, 165329 (2005).  
<sup>28</sup>N. Sugimoto, S. Onoda, S. Murakami, and N. Nagaosa, *Phys. Rev. B* **73**, 113305 (2006).  
<sup>29</sup>K. Nomura, J. Wunderlich, J. Sinova, B. Kaestner, A. H. MacDonald, and T. Jungwirth, *Phys. Rev. B* **72**, 245330 (2005).  
<sup>30</sup>Martin J. Stevens, A. L. Smirl, R. D. R. Bhat, A. Najmaie, J. E. Sipe, and H. M. van Driel, *Phys. Rev. Lett.* **90**, 136603 (2003).  
<sup>31</sup>S. Murakami, N. Nagaosa, and S. C. Zhang, *Phys. Rev. B* **69**, 235206 (2004).  
<sup>32</sup>E. I. Rashba, *Phys. Rev. B* **70**, 161201(R) (2004).  
<sup>33</sup>D. Culcer, J. Sinova, N. A. Sinitsyn, T. Jungwirth, A. H. MacDonald, and Q. Niu, *Phys. Rev. Lett.* **93**, 046602 (2004).

- <sup>34</sup>J. Shi, P. Zhang, D. Xiao, and Q. Niu, Phys. Rev. Lett. **96**, 076604 (2006).
- <sup>35</sup>Q.-F. Sun and X. C. Xie, Phys. Rev. B **72**, 245305 (2005).
- <sup>36</sup>P.-Q. Jin, Y.-Q. Li, and F. C. Zhang, J. Phys. A **39**, 11129 (2006).
- <sup>37</sup>Y. Li and R. Tao, Phys. Rev. B **75**, 075319 (2007).
- <sup>38</sup>R. Shen, Y. Chen, Z. D. Wang, and D. Y. Xing, Phys. Rev. B **74**, 125313 (2006).
- <sup>39</sup>T.-W. Chen, C. M. Huang, and G. Y. Guo, Phys. Rev. B **73**, 235309 (2006).
- <sup>40</sup>H.-T. Yang and C. Liu, Phys. Rev. B **75**, 085314 (2007).
- <sup>41</sup>S. Zhang and Z. Yang, Phys. Rev. Lett. **94**, 066602 (2005).
- <sup>42</sup>Y. Wang, K. Xia, Z.-B. Su, and Z. Ma, Phys. Rev. Lett. **96**, 066601 (2006).
- <sup>43</sup>S. I. Erlingsson, J. Schliemann, and D. Loss, Phys. Rev. B **71**, 035319 (2005).
- <sup>44</sup>C. López-Bastidas, J. A. Maytorena, and F. Mireles, Phys. Status Solidi C **4**, 4229 (2007).
- <sup>45</sup>M. I. D'yakonov and V. I. Perel', Sov. Phys. Solid State **13**, 3023 (1972).